Original/Research Article

OPEN ACCESS

Advances in Engineering and Intelligence Systems

e-ISSN:2821-0263
Volume 03, Issue 03, 2024

Journal Web Page: https://aeis.bilijipub.com

Modeling Compressive Strength of Self-Compacting Concrete (SCC) Using Novel Optimization Algorithm of AOA

Francisca Blanco [1], Ye Ji Woo [2]*

[1] *Faculty of Engineering, University of Mondragon, Arrasate, 20500, Spain*
[2] *Department of Artificial Intelligence, University of Ajou, Suwon-si, Gyeonggi-do, 16499, Republic of Korea*

Highlights

- SCC reduces water use with environmentally friendly components.
- Self-depositing property saves cost and energy by eliminating vibration.
- Novel SVM-based method combined with optimization algorithms.
- High accuracy in predicting SCC compressive strength, R^2 = 97.3%.
- Root means square error (RMSE) of 3.81 MPa indicates effective prediction.

Article Info

Received: 27 July 2024
Received in revised: 10 September 2024
Accepted: 17 September 2024
Available online: 30 September 2024

Keywords

Arithmetic Optimization Algorithm,
Self-Compacting Concrete,
Grasshopper Optimization Algorithm,
Support Vector Regression, Compressive Strength.

Abstract

Self-Compacting Concrete (SCC) has been widely utilized in construction projects and academic research due to its environmentally friendly components, such as fly ash and superplasticizers, which reduce water requirements. SCC's ability to self-deposit eliminates the need for vibration, resulting in cost and energy savings. However, some experts are hesitant about its broader application due to insufficient training in modern materials. Accurately assessing construction aggregates' compressive strength (CS) ensures structural safety. Soft computing methods, which offer a cost-effective and highly accurate alternative to experimental techniques, have attracted interest in modeling dependent variables. This paper presents a novel approach by combining a Support Vector Machine (SVM) with advanced optimization algorithms to estimate the CS of SCC mixtures accurately. The significance of this approach lies in the ability of the optimization algorithms to enhance the performance of the SVM, yielding more precise predictions and addressing the limitations of traditional methods. The developed models were evaluated using several performance metrics, with results showing a strong correlation between predicted and actual values, achieving an R^2 of 97.3%. Furthermore, the root mean square error (RMSE) was calculated at 3.81 MPa, demonstrating the effectiveness of the proposed method in predicting SCC's compressive strength with high accuracy.

Nomenclature

AOA	Arithmetic Optimization Algorithm	*CA*	Coarse Aggregate
CS	Compressive Strength	*C*	Cement
GOA	Grasshopper Optimization Algorithm	*FA*	Fine Aggregate
R2	Coefficient of Determination	*S*	Superplasticizers
RMSE	Root Mean Square Error	*MAE*	Mean Absolute Error
SCC	Self-Compacting Concrete	*W*	Water
SVR	Support vector regression	*Fa*	Fly ash
VAF	Variance Accounted For	*OBJ*	Objective Function

* Corresponding Author: Ye Ji Woo
Email: Acc2Ef2@gmail.com

https://doi.org/10.22034/aeis.2024.470005.1206

1. Introduction

Since prospecting Self Compacting Concrete (SCC) in Japan in the 1980s, a new perspective on concrete technology was brought to the world. SCC was considered a significant event in the construction industry. Introducing SCC gave the critical advances of technologies that have improved concrete quality, improved working conditions in the field, and increased productivity [1]. In this regard, SCC has been attracting attention for its high fluidity due to its weight, which is laid regardless of vibrations. However, it can quickly fill small gaps in the formworks and be pumped over long distances [2]. The usual method for producing Self Compacting Concrete is to confine the content of coarse aggregate associated with a maximum size and mix a low water/binder ratio with a suitable superplasticizer [3].

To attain high fluidity of this concrete and ban the separation and dilution over transporting and placement, compounders used superplasticizer, high Portland cement (PC), and viscosity-adjusting additives [4–6]. Meanwhile, the SCC cost is particularly tied to the using large amounts of chemical materials and cement. For several examples, labor-saving makes it able to have increased costs neutral. On the other side, utilizing original additives, e.g., blast furnace slag, fly ash (FA), and limestone fillers, has reduced SCC ingredient costs and improved concrete freshness and hardening properties [7,8]The literature provides numerous studies on mineral additives that improve compatibility properties and decrease material SCC costs.

Sonebi, in a study [9], made an investigation on SCC incorporating crushed ash of fuel and powder made from limestones that reduced the need for a superplasticizer to have the desired slump rate. Improved rheological properties were also achieved by employing these materials, reducing the concrete risk of cracking from hydrating heat and resulting in durable SCC [10–12]. Bouzoubau and Lachemi, in another research [4], designed an SCC with a large amount to reduce costs. With a water binder ratio of 0.45 and a fly ash cement alternative of 50%, we have produced an economical SCC with a compressive strength of 35 MPa. Ghazel and Khayat found that replacing significant amounts of cement with powdered limestone reduced the cement content required to reach a given slump, viscosity, and compressive strength at an early age [13]. In another research, Nehdi et al. [14] optimized low-cost, high-volume SCC replacement for civil engineering applications. However, replacing up to 50% of cement with a mineral mixture could achieve an economically competitive SCC. In addition, choosing such materials improved further rheological compressive strength and behavior for long spells.

Earning unique characteristics of high-use practical aggregates such as concrete has been controversial in engineering because of various estimating methods: experimental and soft-oriented approaches. This paper has focused on smartly calculating the compressive strength (CS) of the SCC type of concrete.

In one study, an apprising model for CS values used ANFIS and ANN-based models hybridized with the GWO optimization algorithm [15]. Also, Anyaoha et al. estimated the performance of concrete as an HPC type in terms of its CS with various constituents and magnitudes using ten unique models that foresee the CS of concrete samples for 28 days. Finally, outcomes showed that the model of BooST predicted CS values accurately compared to other ways, having the lowest mistake and having an appropriate fitting line in front of experimental target values [16]. Additionally, in a study [17], the Multivariate Adaptive Regression Splines (MARS) model was explored as a feature extraction method to identify the optimal variables for determining the compressive strength of concrete. The extracted features were then fed into a Gradient Boosting Machine (GBM) learning technique to predict the compressive strength.

Further research as a comparative study was conducted using a model, namely, regression of kernel ridge and Gaussian, to examine their robustness. A total data set of 8 input ingredients, including blast furnace slag, cement, superplasticizer, water, fine aggregate, and age of concrete, were used as the entering variables for estimating the compressive strength of HPC. The analysis results illustrated the importance of the weight used for ingredients in the process of GBM; however, the coefficient of correlation and mean absolute error were obtained, respectively, at 0.971 and 0.0372 MPa.

Consequently, the present research aims to model the CS values of SCC concrete samples, in which several ingredients include cement, water, fly ash, coarse aggregate, fine aggregate, and superplasticizer. The samples must be fed to support vector regression (SVR) as the primary model to predict the CS values based on inputs. Using SVR to train a dataset of variables and targets for reproducing targets is the smart approach to replacing experimental ways found in many references [18–21]. The novelty of this research lies in the application of the Grasshopper Optimization Algorithm (GOA) and Arithmetic Optimization Algorithm (AOA) to enhance the predictive performance of the Support Vector Machine (SVM) model for estimating the compressive strength (CS) of Self-Compacting Concrete (SCC). These optimization algorithms contribute uniquely by fine-tuning the SVM model parameters, addressing the complex nonlinear relationships in SCC mixtures more effectively than conventional approaches. This combination improves the model's accuracy, enabling more precise CS predictions. By leveraging these advanced algorithms, the study introduces a robust and efficient method for optimizing machine learning models in concrete strength estimation. The abovementioned approaches have been used prospectively in research [22–27]. In this regard, Fig. 1 shows the study flowchart. The following sections will define the primary model of SVR and coupling optimizers, and some criteria will be used to assess their results.

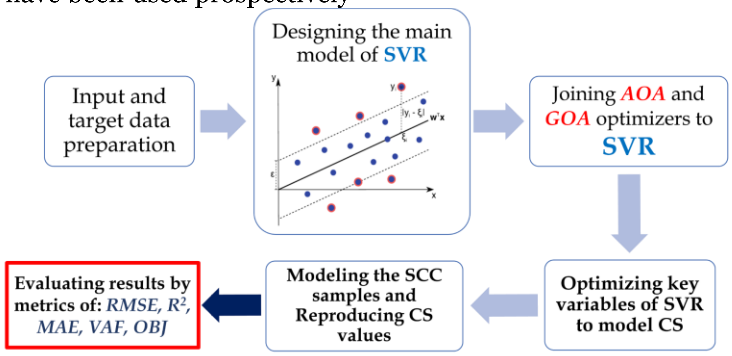

Fig. 1. Flow chart of the research

2. Methodology

2.1. Support Vector Machine (SVM): Main model of Estimation

SVM, designed via Vapnik (1995) [28], has many abilities in predicting and finding patterns and minimizing error rates to reduce complexity and cost. This approach can find optimal answers uniquely and globally. Recently, this method has been applied successfully in many problems of civil engineering [18,29–32]. The vital objective of SVM is determined to locate the unprocessed dataset into a multi-dimensional area that fits a function linearly with lower logical complexity to the space specified [33,34]. The second phase tries to create the function as flat as possible to decrease the complexities, i.e., better generalizing for having a substantial extent.

$XY = \{(x, y) \mid (x_1, y_1), \ldots, (x_n, y_n)\}$ are the training cases with the number of training samples shown by n. By considering the linear form of SVR, the connection of the target of x_k with $\hat{y}_k$ as the predicted variable would be defined as the linear relation in Eq. (1):

$$\hat{y}_k = f(x_k) = \langle w, x_k \rangle + b \quad (1)$$

where b and w as the bias vector and weight vector, respectively, play the leading roles; the symbol $\langle .,. \rangle$ is showing the dot production function. Finding unknown vectors of (w, b) reduces the errors for samples with ε deviation from y_k as a target. That second concept of deviation affirms that by existing ε-intensive cost function of $|y_k - f(x)| \leq \varepsilon$, the formulation given l_ε is brought in Eq. (2):

$$l_\varepsilon = |y_k - f(x)|_\varepsilon = max\{0, |y_k - f(x)| - \varepsilon\} \quad (2)$$

To have an optimal SVM rate, the norm of w, $\|w\|^2 = \langle w, w \rangle$ must be minimized to ensure that the lowest complexity risk is reached. Therefore, the constrained regression problem in mathematical terms can be rewritten as follows in Eq. (3):

$$min_{w,b} = \frac{1}{2}\|w\|^2 + C\sum_{i=1}^{m}(\xi_i + \xi_i^*) \quad (3)$$

$$constraints \begin{Bmatrix} y_i - (w^T x_i + b) \leq \varepsilon + \xi_i \\ (w^T x_i + b) - y_i \leq \varepsilon + \xi_i^* \\ \xi_i, \xi_i^* \geq 0 \end{Bmatrix}$$

whereby, in equation (10), w is the weight factor, bias is demonstrated by b; regularization parameter in the queue is shown by C; boundary violation is assigned with ξ; the deviation from the hyperplane is indicated by ε. Using the Lagrange method, the presented formula in Eq. (3) can be solved using a convex quadratic programming optimization using the positive Lagrange multiplier variable sets. By maximizing its dual optimization problem, the mentioned function would be solved with saddle point given the dual and primary variables that are defined as follows:

$$w = \sum_{k=1}^{n}(\alpha_k - \alpha_k^*)x_k \rightarrow \hat{y}_{new} = f(x_{new}) = \sum_{k=1}^{n}(\alpha_k - \alpha_k^*)\langle x_k, x_{new} \rangle + b \quad (4)$$

Lagrange multipliers are α_k and α_k^* equal or more than zero. Dealing with the non-linear complex models for the relations between inputs and outputs domains, procedures of training patterns can do pre-processing [33,35]. That mapping inputs into a multi-dimensional space with the aid of kernel functions yields the SVM non-linear for the kernel function of $k\langle .,. \rangle$. Continuously as mentioned, computing the $bias$ and $weight$ is required operation that in the quadratic objective function reaching the desired parameters (C, ε and $sigma$) of SVR at the optimal levels would be a problem needs to be optimized by algorithms that is defined in next section [36]. Fig. 2 illustrates the flowchart of the SVR model.

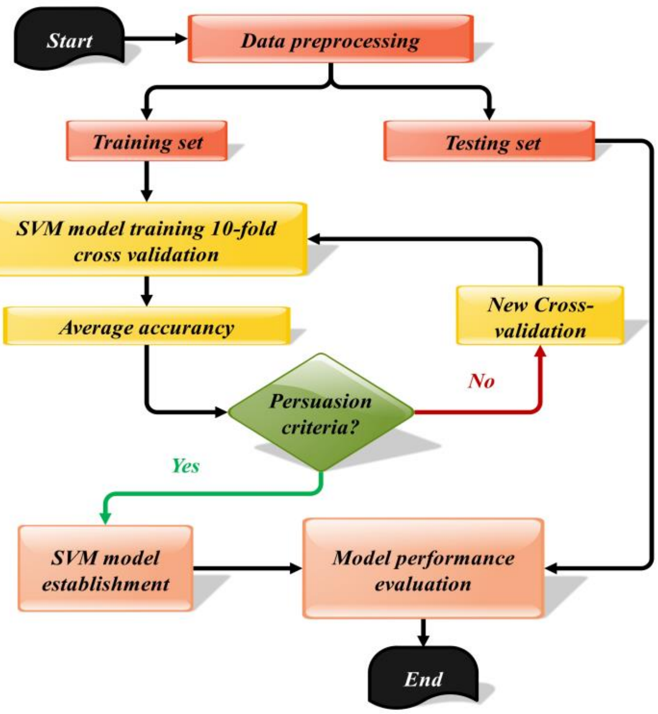

Fig. 2. Flow chart of the SVR model

I) Arithmetic Optimization Algorithm (AOA)

The arithmetic optimization algorithm is known as AOA, including algebraic notion as the arithmetic operators that are a candidate-based method for searching plus updating the new places of the population without considering corresponded derivatives [37]. Mathematical approaches are meant by arithmetic, which are critical sections, such as the theories on algorithm's procedure initializing candidates randomly for an optimal solution.

$$C = \begin{bmatrix} c_{1,1} & \cdots & c_{1,j} \\ \vdots & \ddots & \vdots \\ c_{N,1} & \cdots & c_{N,j} \end{bmatrix} \tag{5}$$

Explorating and exploiting operations compose the critical sectors of this approach. Subsequently, the exploration searching area or exploiting should be conducted after producing the initial candidates that employ the accelerator of math optimizer (MOA) functions.

$$MOA = Min + iter \times (\frac{Max - Min}{Max_{iter}}) \tag{6}$$

That Max and Min denote the MOA maximum and minimum rates; The variable representing the maximum iteration number is Max_{iter}; and the number of the current iteration is determined by the variable of $iter$.

AOA owns the basic arithmetic operators multiplying (M) and dividing (D), processing the exploration search phase. Using referred operators accelerates reaching target performance while employing arithmetic operators subtracting (S) and adding (A) in the exploiting step will attain the optimal answer.

AOA way will do its tasks in the exploration step if $MOA < r_1$. The position would be updated in the exploration step via relation 7, which uses the dividing (D) multiplying (M) operators.

$$c(iter+1)_{i,j} = \begin{cases} best(c_j) \div (MOP + \varepsilon) \times ((ub - lb) \times \mu + lb\ ) & r_2 > 0.5 \\ best(c_j) \div (MOP) \times ((ub - lb) \times \mu + lb\ ) & otherwise \end{cases} \tag{7}$$

Where ε equals a small number, μ is the adjusting parameter to be used in the locating answer that equals at 0.499 level; the best global place of the answer is shown via $best\ (c_j)$; ub and lb are the up and bottom boundary of the area for search, and for computing, the factor of MOP below relation is to help.

$$MOP(iter) = 1 - \frac{iter^{1/\alpha}}{Max_{iter}{}^{1/\alpha}} \tag{8}$$

In relation (8), the variable of α shows the exploiting sensitivity and accuracy in epochs that are determined 5

$$c(iter+1)_{i,j} = \begin{cases} best(c_j) - (MOP) \times ((ub - lb) \times \mu + lb\ ) & r_3 > 0.5 \\ best(c_j) + (MOP) \times ((ub - lb) \times \mu + lb\ ) & otherwise \end{cases} \tag{9}$$

[25–27]. Notably, ($r_{1,2,3}$) numbers of random pseudo are distributed uniformly in the [zero to 1].

The search area when MOA<r_1 forms via the operators of D and M; however, area search by the operators of addition (A) and subtraction (S) would be in the exploration phase if MOA≥r_1. Subsequently, the search process will be done as shown in the following relation. The flowchart of the AOA is presented in Fig. 3.

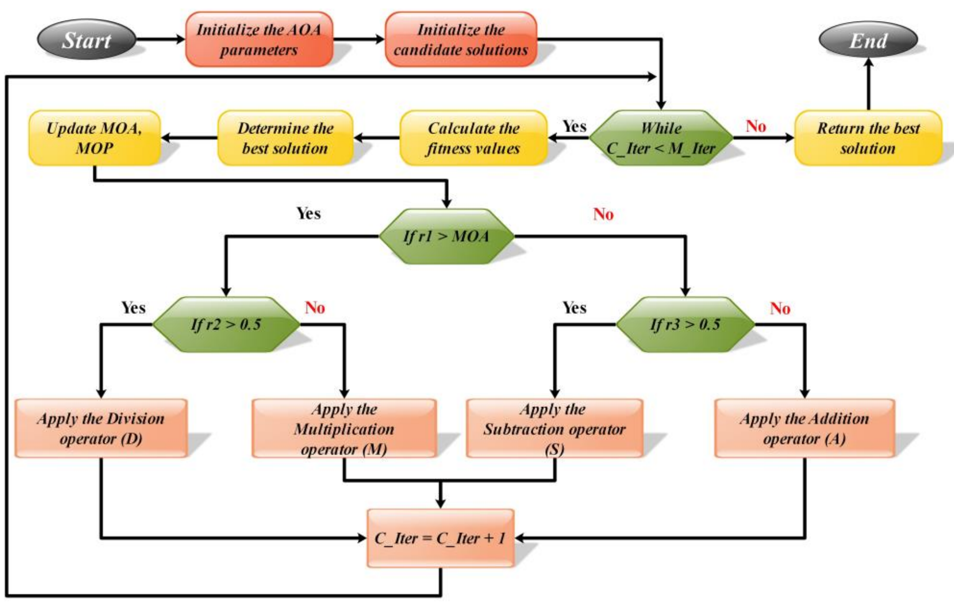

Fig. 3. Flow chart of the AOA

II) Grasshopper Optimization Algorithm (GOA)

The grasshopper behavior in nature to find food is similar to many algorithms that were developed, such as the whale optimization algorithm (WOA), the salpa swarm algorithm, and the ant lion optimizer (ALO) [38], has inspired the researchers to introduce the Grasshopper Optimization Algorithm (GOA) for optimizing problems [39]. Two determining stages of exploiting and exploring are involved for GOA optimizer identical to AOA but here for looking for food. The grasshoppers fly on various scales in the local and global areas, searching for foods [39]. Characteristics of long-way and sudden movement are recognizable throughout the adulthood of these tiny insects' heads. The formula form of the mentioned characteristics of grasshoppers is defined in the following relation:

$$x_i = S_i + A_i + G_i \tag{10}$$

where, x_i represents the grasshopper i place. Respectively, the interactions of the insects in their regions can be expressed as written in relation (11).

$$S_i = \sum_{\substack{j=1 \\ i \neq j}}^{N} s(d_{ij})\hat{d}_{ij}\ , \quad d_{ij} = |x_i - x_j|\ ,\ \hat{d}_{ij} = \frac{x_i - x_j}{d_{ij}} \tag{11}$$

For this relation, the distance of insects representing i and j has been shown via d_{ij}The parameter showing insects' interactions is S_i; in addition, $\hat{d}_{ij}$ variable demonstrates the vector that is unit and places between insects i toward j. On the other side, the social force of insects is formulated in Eq. (11).

$$s(x) = fe^{\frac{-x}{l}} - e^{-x} \tag{12}$$

Where s shows the social force of insects; the intensity of attraction is indicated by f, and l represents the drawing length. Wind and gravity are important factors for these insects in nymph steps that influence their flying with no wings using Eq. (13). These items are calculated.

$$A_i = u\hat{e}_w\,, \quad G_i = -g\hat{e}_g \tag{13}$$

Wherein wind movement direction has been shown by A_i; the gravity factor is considered for grasshoppers i by G_i. The unit vectors of $\hat{e}_w$ and $\hat{e}_g$ define the directions of winds and gravity force, respectively. Wind drift and gravity regulator constants are shown with u and g. Finally, rewritten relation (10) can be illustrated as brought up in Eq. (14):

$$X_j^d = c\left[\sum_{\substack{j=1\\ i\neq j}}^{N} c\,\frac{ub_d - lb_d}{2}\, s\left(\left|x_i^d - x_j^d\right|\right)\frac{x_i - x_j}{d_{ij}}\right] + \widehat{D}_d \tag{14}$$

ub_d and lb_d are the symbols of up and bottom boundaries; $\widehat{D}_d$ is the dimensions' rate of distances among grasshoppers; N represents the number of populations; decremental coefficient is depicted via c that declines by increasing iterations in creating the balance between the exploration and exploitation stages. In this respect, the following relation is written to improve the exploitation phase:

$$c = c_{max} - Iter \times \frac{c_{max} - c_{min}}{M.Iter} \qquad \begin{cases} c_{max} = 1 \\ c_{min} = 0.0001 \end{cases} \tag{15}$$

Fig. 4 shows the flowchart of the GOA.

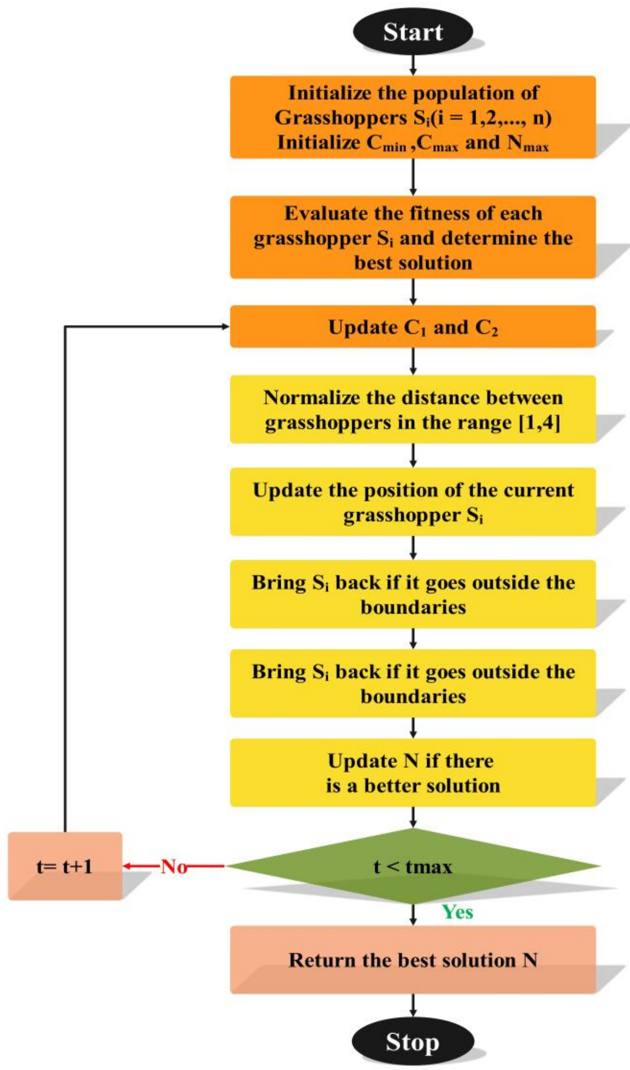

Fig. 4. Flow chart of the GOA

2.2. *Justification of model*

Support Vector Regression (SVR) was selected as the sole model for predicting the compressive strength (CS) of Self-Compacting Concrete (SCC) in this study due to its superior ability to manage the complex, nonlinear relationships inherent in the factors influencing CS. The compressive strength of SCC is affected by multiple interacting variables, such as the water-cement ratio, aggregate properties, and admixture content, all exhibiting nonlinear behavior. SVR's proficiency in handling these nonlinearities and capturing intricate patterns within the data makes it particularly well-suited for this prediction task. The decision to exclusively utilize SVR was further supported by its strong performance in preliminary analyses, where it consistently outperformed other models regarding accuracy and reliability. When integrated with novel optimization algorithms, SVR demonstrated exceptional predictive accuracy and stability, highlighting its potential for real-world applications in construction. Focusing solely on SVR allowed the study to deeply optimize this model, resulting in finely tuned parameters that enhanced its predictive power. This targeted approach provided a thorough understanding of SVR's capabilities and limitations, enabling significant advancements in the accuracy of CS predictions. By concentrating on SVR, the research achieved reliable and robust predictions and contributed to the development of optimized methodologies that can be applied to other complex prediction problems in civil engineering.

2.3. *Hyperparameters*

Table 1 shows the hyperparameter tuning results in two SVR models: A-SVR and G-SVR. The hyperparameters tuned for both models are the regularization parameter C, the epsilon value in the loss function, and the kernel coefficient gamma. The optimized parameters with the A-SVR model are C = 3.04219, epsilon = 1, and gamma = 47. Such values indicate that the A-SVR model has been tuned to balance the divergent goals of maximizing the margin while minimizing training error; the high value of gamma also shows a strong influence of individual data instances in defining this model's decision boundary. In contrast, the G-SVR model had different hyperparameters, notably C = 2.17348, epsilon = 1, and gamma = 23. The lower gamma value means that the G-SVR model depends on a larger span of data points to define its separating hyperplane, which can yield a smoother prediction surface. These differences in hyperparameter values point towards different optimizations for both models to capture nonlinear relationships within the data. Among them, C, epsilon, and gamma are the most critical parameters that can balance model complexity and performance for SVR models and, therefore, the accuracy of prediction of the CS of SCC.

Table 1. The results of hyperparameters

Models	Hyperparameter		
	C	Epsilon	Gama
A-SVR	3.04219	1	47
G-SVR	2.17348	1	23

2.4. *Evaluation indicators for hybrid models*

By coupling the primary model SVR and optimization algorithms of AOA and GOA, the produced hybrid models should be assessed based on the generated results. In this regard, the following relations evaluate the results and allow us to compare results.

$$RMSE = \sqrt{\frac{1}{N}\sum_{n=1}^{N}(t_n - p_n)^2} \tag{16}$$

$$R^2 = \left(\frac{\sum_{n=1}^{N}(t_n - \bar{t})(p_n - \bar{p})}{\sqrt{[\sum_{n=1}^{N}(t_n - \bar{p})^2][\sum_{n=1}^{N}(p_n - \bar{p})^2]}}\right)^2 \tag{17}$$

$$VAF = \left(1 - \frac{var(t_n - p_n)}{var(t_n)}\right) * 100 \tag{18}$$

$$OBJ = \left(\frac{n_{train} - n_{test}}{n_{train} + n_{test}}\right)\frac{RMSE_{train} + MAE_{test}}{R_{train}^2 + 1} + \left(\frac{2n_{train}}{n_{train} + n_{test}}\right)\frac{RMSE_{test} - MAE_{test}}{R_{test}^2 + 1} \tag{19}$$

$$MAE = \frac{1}{N}\sum_{n=1}^{N}|p_n - t_n| \tag{20}$$

In the abovementioned relations, observed and predicted compressive strength numbers are, alternatively, illustrated by t_n and p_n; The variance account factor index has been shown by VAF; the root mean squared error formula is depicted by $RMSE$; the parameters of $n_{training}$ and $n_{testing}$ show the SCC samples' number for the train and test stages; correlation index of R^2 is for observed (as target) and modeled CSs, the whole samples number is demonstrated via N; the mean absolute error index is

MAE; $\bar{t}$ is showing the mean value of measured CS and $\bar{p}$ denote that of predicted CS.

2.5. Preparing hybrid models and calibration

Compressive strength modeling for SCC mixtures using SVR is coupled with the introduction of optimizing algorithms such as the hybrid A-SVR and G-SVR models. 327 SCC samples dataset was considered for this research, including ingredients rates plus the age of concrete samples measuring given CS gathered from published reference [40], and Table 2 indicates the data summary in terms of statistical viewpoints. These data are divided into two kinds: i) independent parameters such as ingredients mixed to produce SCC mixtures plus their ages, and ii) dependent parameters as the target values that are compressive strength influenced by various rate data i. All data feed hybrid A-SVR and G-SVR models as training and validating phases, after which they are tested. However, the three phases mentioned are done in the training phase as sub-phases. Notably, 70% of the samples' data will be used in the training stage, and the other 30% will be employed for testing and validating phases at the same percentage.

By training models with all independent and dependent (target) parameters of 70% of all samples, the 15% of data, again including dependent and independent parameters, will be used to validate model results by comparing the estimated CS values and measured ones, leading to fixing the weights and biases rates. In the last stage of the test, the remaining 15 percent of data are investigated with actual experimental data. However, just independent variables are used here, with w and b rates determined in the previous section [41]. Fig. 5 indicates the dataset as input variables, including CS and ingredients of SCC samples, plus the age of concretes in which the compressive strength is recorded.

Table 2. The summary of data used for training models

Component	Nomenclature	Max	Min	Ave	St. dev.
Cement	CE (kg/m3)	503	61	293.08	89.78
Water	WA (kg/m3)	390.39	132	197	37.62
Fly ash	FA (kg/m3)	373	20	170.23	69.68
Coarse Aggregate	CA (kg/m3)	1190	590	828.34	137.3
Fine Aggregate	FG (kg/m3)	1109	434	807.47	135.8
Superplasticizers	SP (kg/m3)	113.55	0	23.15	27.09
SCC sample age	Age (days)	365	1	44.31	63.76
Compressive Strength	CS (MPa)	90.6	4.44	36.45	19.07

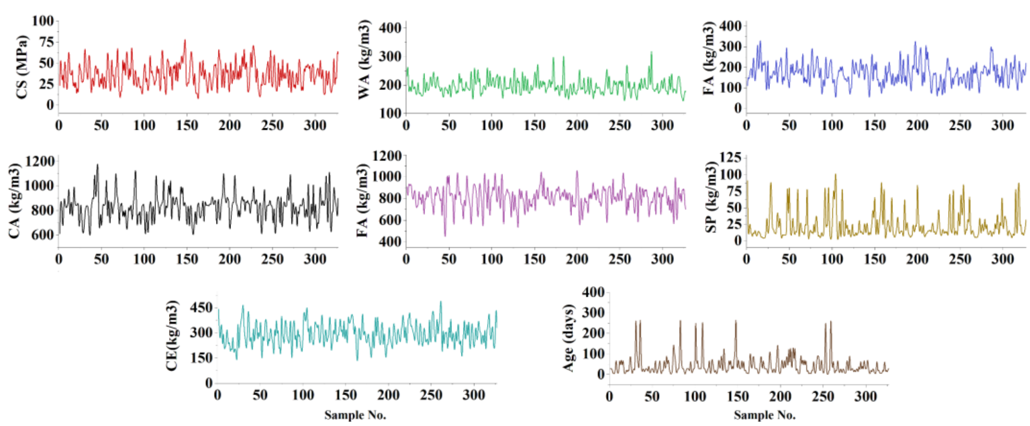

Fig. 5. Inputs and target data fed to models for training and validation

3. Results and discussions

This section will investigate the A-SVR and G-SVR models in generating the CS values for SCC samples based on input variables. The fundamental data of ingredients and age of mixtures as the initial entering data are considered in three phases: training, validation, and testing. The primary support vector regression model (SVR) coupled with the AOA and GOA were optimized in calculating *C*, *Epsilon (ε),* and *sigma*. Fig. 6 shows the compressive strength rates measured in the experimental process as target values and a benchmark to assess results.

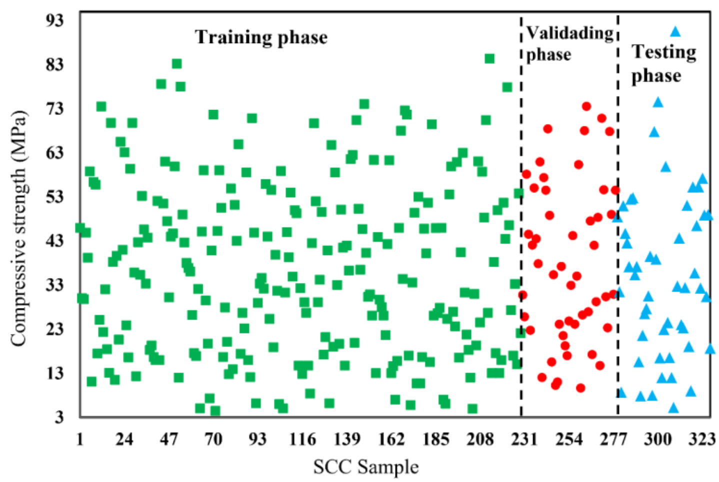

Fig. 6. Compressive strength rates measured as target rates

Fig. 7 shows the CS Values modeled by A-SVR and G-SVR to start the evaluation. As mentioned in Fig. 7, the two hybrid frameworks have calculated the CS rates with diverse mechanisms. Consequently, the outcomes of the models differ, which has led to creating these bar charts with different bars.

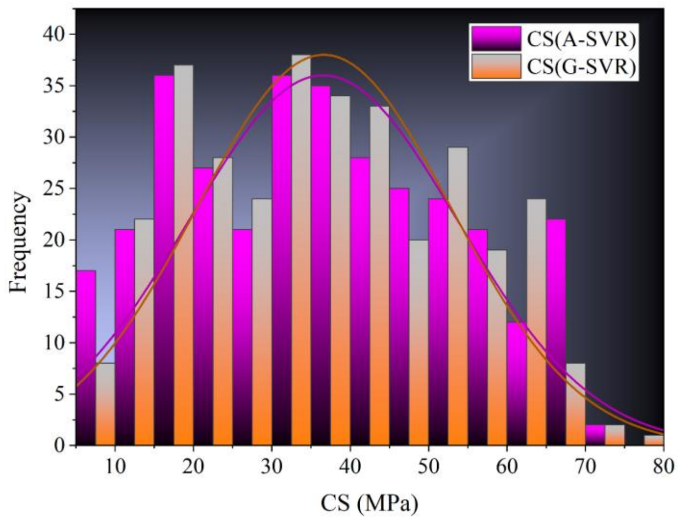

Fig. 7. The CS rates produced by models A-SVR and G-SVR

However, the standard distribution curve of G-SVR is sharpened, showing that the spreading CS rates are widely projected. At the same time, the A-SVR is flatter, implying that CSs have a higher concentration for determining reaches. Notably, the CS rates with the values 15-20 and 30-35 MPa comprise most of the data generated by models. In this regard, errors that can cause different data will always accompany the modeling process. To show the errors, Fig. 8 indicates the error of each sample considering the modeled and target rates for A-SVR and the CS rates in front of each mixture.

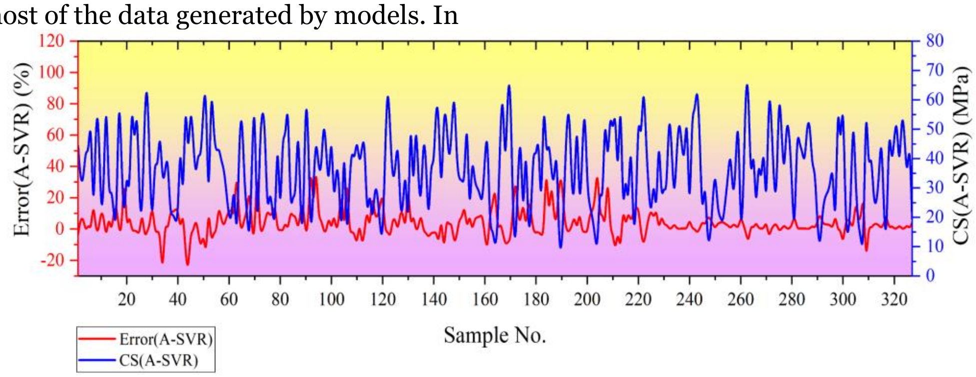

Fig. 8. The error rates and CS modeled by A-SVR

Accordingly, the error rates are seen with no regular pattern, but at first glance, the errors are in the training phase. In contrast, in the validation stage, the errors have been reduced, but again, in testing, the errors have tended to increase. In a model with an AOA optimizer, the mixtures with the number of 19 have a 39.72% error, 44 have a 29.17% error, 63 have a 41.65% error, 71 have 46.90%, 94 have a 46.48% error, 106 have a 41.65%, 184 having 47.05%. Fig. 9 shows the error rates and CS modeled by G-SVR in comparison with A-SVR, we can see the harsh diagram with a high rate of fluctuations, especially for the mixtures reaching the 100% error rates. There is not any constant pattern in distribution errors in the three phases.

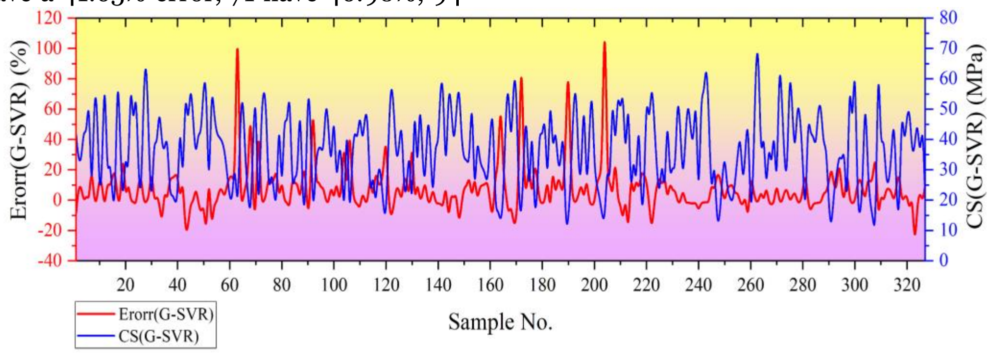

Fig. 9. The error rates and CS modeled by A-SVR

To better understand the capability of developed frameworks in modeling the compressive strength of SCC samples, Table 3 tries to give the assessment results of several indicators used in this research. As shown in Table 3, the results of CS models are evaluated in four stages. Besides the three phases presented before, all conditions are applied to consider all the data in one phase to give the overall view of the model's performance. Regarding the indicators provided, the correlation of CS values as modeled and measured in the testing phase favored G-SVR with a 1.54% difference. At the same time, in the same condition, the A-SVR could obtain 97.32 percent for the same condition R^2 in the training phase is 0.31 percent higher than G-SVR. Also, the outputs of RMSE showed the malfunction of G-SVR in modeling CS values despite the lower rate of this index for A-SVR in all conditions, with a 17.69 % difference. Interestingly, in the testing stage, the GOA could tune the SVR better than AOA with RMSE of 2.93 and 3.77 MPa, respectively.

Also, MAE has a better result for A-SVR in the training phase than G-SVR. There is a 23.63% discrepancy between models. Nevertheless, this pattern in other stages runs in results. Moreover, the VAF index performed an assessment operation to show the irregular status of models in different phases. For example, in the validating and testing stages, the G-SVR is of higher performance, 98.73 and 98.72, respectively, and in the remaining phases, A-SVR is the model with better simulation results. The highest difference rate between the VAF of models happened in the test stage with 2 percent.

Table 3. The results of assessing criteria

		Indexes				
		RMSE	**R2**	**MAE**	**VAF**	**OBJ**
A-SVR	Train stage	3.679716	0.973285	2.450206	98.00863	-
	Test stage	3.771117	0.971102	1.343838	96.79443	-
	Validation	3.810161	0.970987	1.36944	97.70135	-
	All	3.504594	0.974614	2.091095	97.86734	2.901549
G-SVR	Train stage	4.481954	0.97027	3.029129	97.11676	-
	Test stage	2.93278	0.986082	1.91798	98.72903	-
	Validation	2.96034	0.985964	1.939242	98.72341	-
	All	4.124493	0.97169	2.710418	97.39398	3.26344

Additionally, the OBJ indicator, as the comprehensive criterion, encompasses all indicators of R^2, RMSE, and MAE in whole phases, evaluated the CS rates generated by A-SVR and G-SVR with the better performance for a former model with a 12.47% difference. For analyzing the correlation of CS modeled and measured for models, Fig. 10 indicates the fitting lines and given line equation. The slope and intersect exhibit the modeling process being near the target values. As mentioned in Fig. 10, both models could simulate the mechanical behavior of SCC samples near the Y=X line as the target line. Meanwhile, the performance of AOA (a) in optimizing SVR has been more potent than

GOA. By the points of CS near the bisector Y=X, there are many cases in GOA where the points are in farther positions than AOA. This fact has led to a different slope for models. Concerning correlation rate, this fact is actual that the slope rate of G-SVR by 0.839 values is 4.5 percent lower than A-SVR with a slope rate of 0.88. Conversely, the R^2 correlation index proves that the AOA has been more successful than GOA, with a 0.3% MPa difference.

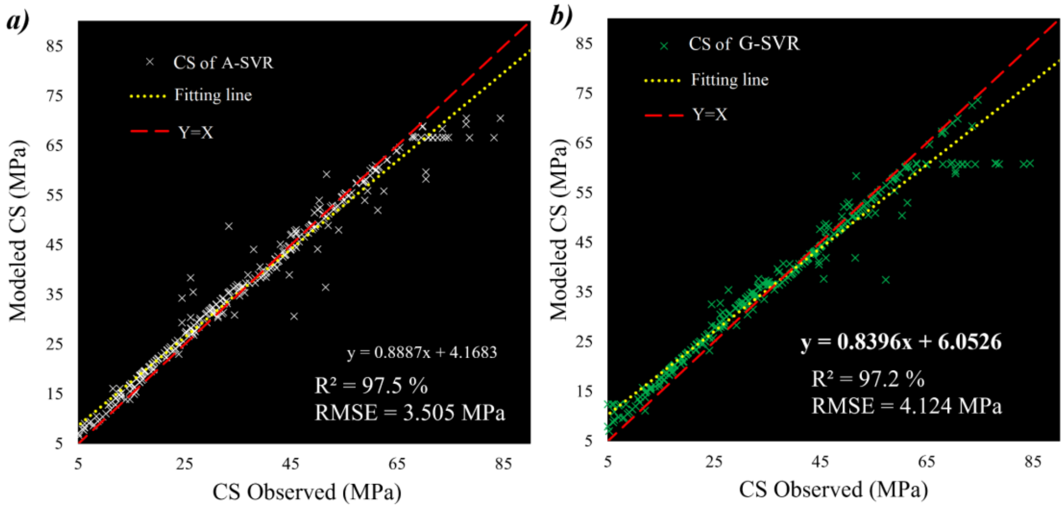

Fig. 10. The plots of CS measured against the modeled by a) A-SVR and b) G-SVR

Fig. 11 highlights the existing differences in model outputs. It indicates the discrepancy between CS modeled by A-SVR and G-SVR. As shown in Fig. 11, the differences between models in simulating the CS of SCC samples can be found in many cases, especially for the validation and training phases. At the same time, it has been better in the testing phase.

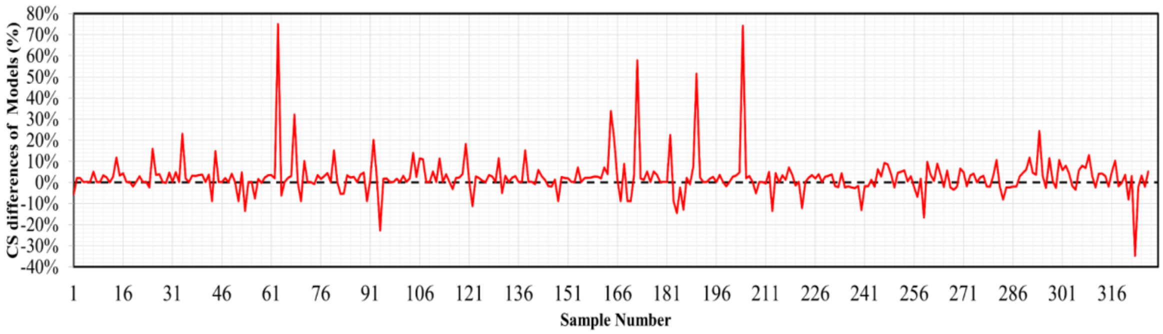

Fig. 11. The difference in CS rates modeled by AOA-SVR and GOA-SVR

4. Conclusion

Self-compacting concrete (SCC) has been adopted worldwide in many construction and academic research projects. SCC includes environmentally friendly materials like fly ash and superplasticizers, reducing the required water. Being self-deposited results in no need for vibration, saving capital and energy. Introducing SCC gave rise to critical advances in technologies that have improved concrete quality, improved working conditions in the field, and increased productivity. In this regard, SCC has been attracting attention for its high fluidity due to its weight, which is laid regardless of vibrations.

Meanwhile, the SCC cost is particularly tied to the using large amounts of chemical materials and cement. For several examples, labor-saving makes it able to have increased costs neutral. Appraising compressive strength (CS) of constructional aggregates has been vital in estimating structures' safety. Therefore, using soft computing methods as economical compared to experimental ones and highly high-accurate has inspired researchers to investigate intelligent procedures in modeling the dependent variables. Machine learning methods have attracted attention for modeling concrete features, especially CS. Thus, this paper aims to model the CS of SCC mixtures using a support vector machine coupled with Grasshopper (GOA) and Arithmetic optimization algorithms (AOA) to estimate the CS values accurately. In this regard, the correlation of CS values modeled and measured in the testing phase favored G-SVR with a 1.54% difference, while in the same condition, the A-SVR obtained 97.32 percent for R2 in the training phase was 0.31 percent higher than G-SVR. Also, the outputs of RMSE showed the malfunction of G-SVR in modeling CS values despite the lower rate of this index for A-SVR in all conditions, with a 17.69 % difference.

Interestingly, in the testing stage, the GOA could tune the SVR better than AOA with RMSE of 2.93 and 3.77 MPa, respectively. Also, MAE has a better result for A-SVR in the training phase than G-SVR. There is a 23.63% discrepancy between models. Nevertheless, this pattern in other stages runs in results. The differences in models' results in simulating the CS of SCC samples were found in several points. Finally, with the higher capability of modeling CS and controlling errors, the AOA was a highly accurate solution to optimize the problem compared to GOA.

- **Limitation**

This study, while providing valuable insights into modeling the compressive strength (CS) of Self-Compacting Concrete (SCC) using Support Vector Regression (SVR) optimized by Grasshopper Optimization Algorithm (GOA) and Arithmetic Optimization Algorithm (AOA), has certain limitations. Firstly, the dataset used, although comprehensive, may not fully capture the variability of SCC mixtures in diverse environmental conditions and with different material properties. This limitation could affect the generalizability of the model to broader applications. Secondly, the study relies on SVR as the sole machine learning technique, which, despite its robustness, might not outperform other advanced models or hybrid approaches in all scenarios. Additionally, while effective, the optimization algorithms have parameters that require careful tuning, which may limit their applicability to other optimization problems. Future research should explore different machine learning models and larger datasets to validate and extend the findings.

- **Future study**

Building on the findings of this study, several avenues for future research can be pursued to enhance the modeling of CS of SCC. First, expanding the dataset by incorporating a more comprehensive range of SCC mixtures, including those with different aggregate types, admixtures, and curing conditions, would help improve the model's generalizability and robustness. Future studies could also explore integrating other advanced machine learning models, such as deep learning techniques or ensemble methods, to outperform the SVR model used in this study potentially. Additionally, further research could investigate the impact of hybrid optimization algorithms that combine the strengths of multiple algorithms to optimize the model more effectively. Exploring real-time optimization techniques, where models are continuously updated with new data, could also benefit practical applications in the construction industry. Moreover, evaluating the environmental and economic impacts of using these optimized models in real-world construction projects would provide valuable insights into their practical benefits. Finally, collaboration with industry stakeholders to apply these models in actual construction projects could validate the findings and demonstrate the practical utility of the proposed approach.

Conflicts of Interests: There is no conflict of interest in this study.

Funding: Self-funded.

Acknowledgments: Not applicable.

Availability of Data and Materials: The datasets used during the current study are available from the corresponding author on request.

Using Artificial Intelligent Chatbots: None.

References

[1] Zhu W, Bartos PJM. Permeation properties of self-compacting concrete. Cem Concr Res 2003;33:921–6.

[2] Phan TH, Chaouche M, Moranville M. Influence of organic admixtures on the rheological behaviour of cement pastes. Cem Concr Res 2006;36:1807–13.

[3] Okamura H, Ouchi M. Self-compacting concrete. Journal of Advanced Concrete Technology 2003;1:5–15.

[4] Sari M, Prat E, Labastire J-F. High strength self-compacting concrete original solutions associating organic and inorganic admixtures. Cem Concr Res 1999;29:813–8.

[5] Sakata N, Maruyama K, Minami M. 20 basic properties and effects of welan gum on self-consolidating concrete. Production Methods and Workability of Concrete 2004;32:237.

[6] Lachemi M, Hossain KMA, Lambros V, Nkinamubanzi P-C, Bouzoubaa N. Performance of new viscosity modifying admixtures in enhancing the rheological properties of cement paste. Cem Concr Res 2004;34:185–93.

[7] Şahmaran M, Christianto HA, Yaman İÖ. The effect of chemical admixtures and mineral additives on the properties of self-compacting mortars. Cem Concr Compos 2006;28:432–40.

[8] Bouzoubaâ N, Lachemi M. Self-compacting

concrete incorporating high volumes of class F fly ash: Preliminary results. Cem Concr Res 2001;31:413–20.
[9] Sonebi M. Medium strength self-compacting concrete containing fly ash: Modelling using factorial experimental plans. Cem Concr Res 2004;34:1199–208. doi:10.1016/j.cemconres.2003.12.022.
[10] Sonebi M, Bartos PJM. Filling ability and plastic settlement of self-compacting concrete. Mater Struct 2002;35:462–9.
[11] Khurana R, Saccone R. Fly ash in self-compacting concrete. Special Publication 2001;199:259–74.
[12] Khayat KH, Bickley J, Lessard M. Performance of self-consolidating concrete for casting basement and foundation walls. Materials Journal 2000;97:374–80.
[13] Ghezal A, Khayat KH. Optimizing self-consolidating concrete with limestone filler by using statistical factorial design methods. Materials Journal 2002;99:264–72.
[14] Nehdi M, El Chabib H, El Naggar MH. Development of cost-effective self-consolidating concrete for deep foundation applications. Concrete International, American Concrete Institute 2003;25:49–57.
[15] Golafshani EM, Behnood A, Arashpour M. Predicting the compressive strength of normal and High-Performance Concretes using ANN and ANFIS hybridized with Grey Wolf Optimizer. Constr Build Mater 2020;232:117266. doi:10.1016/j.conbuildmat.2019.117266.
[16] Anyaoha U, Zaji A, Liu Z. Soft computing in estimating the compressive strength for high-performance concrete via concrete composition appraisal. Constr Build Mater 2020;257:119472. doi:10.1016/j.conbuildmat.2020.119472.
[17] Kaloop MR, Kumar D, Samui P, Hu JW, Kim D. Compressive strength prediction of high-performance concrete using gradient tree boosting machine. Constr Build Mater 2020;264:120198.
[18] Pal M, Deswal S. Support vector regression based shear strength modelling of deep beams. Comput Struct 2011;89:1430–9.
[19] Cheng M-Y, Prayogo D, Wu Y-W. Novel genetic algorithm-based evolutionary support vector machine for optimizing high-performance concrete mixture. Journal of Computing in Civil Engineering 2014;28:6014003.
[20] Shamshirband S, Petković D, Amini A, Anuar NB, Nikolić V, Ćojbašić Ž, Kiah MLM, Gani A. Support vector regression methodology for wind turbine reaction torque prediction with power-split hydrostatic continuous variable transmission. Energy 2014;67:623–30.
[21] Chou J, Pham A. Smart artificial firefly colony algorithm-based support vector regression for enhanced forecasting in civil engineering. Computer-Aided Civil and Infrastructure Engineering 2015;30:715–32.
[22] Luo J, Chen H, Xu Y, Huang H, Zhao X. An improved grasshopper optimization algorithm with application to financial stress prediction. Appl Math Model 2018;64:654–68.
[23] Mafarja M, Aljarah I, Heidari AA, Hammouri AI, Faris H, Ala'M A-Z, Mirjalili S. Evolutionary population dynamics and grasshopper optimization approaches for feature selection problems. Knowl Based Syst 2018;145:25–45.
[24] Zhang X, Miao Q, Zhang H, Wang L. A parameter-adaptive VMD method based on grasshopper optimization algorithm to analyze vibration signals from rotating machinery. Mech Syst Signal Process 2018;108:58–72.
[25] Agushaka JO, Ezugwu AE. Advanced arithmetic optimization algorithm for solving mechanical engineering design problems. PLoS One 2021;16:e0255703. doi:10.1371/journal.pone.0255703.
[26] Khatir S, Tiachacht S, Le Thanh C, Ghandourah E, Mirjalili S, Abdel Wahab M. An improved Artificial Neural Network using Arithmetic Optimization Algorithm for damage assessment in FGM composite plates. Compos Struct 2021;273:114287. doi:10.1016/j.compstruct.2021.114287.
[27] Abualigah L, Almotairi KH, Abd Elaziz M, Shehab M, Altalhi M. Enhanced Flow Direction Arithmetic Optimization Algorithm for mathematical optimization problems with applications of data clustering. Eng Anal Bound Elem 2022;138:13–29.
[28] Cortes C, Vapnik V. Support-vector networks. Mach Learn 1995;20:273–97.
[29] Chen B-T, Chang T-P, Shih J-Y, Wang J-J. Estimation of exposed temperature for fire-damaged concrete using support vector machine. Comput Mater Sci 2009;44:913–20.
[30] Lute V, Upadhyay A, Singh KK. Support vector machine based aerodynamic analysis of cable stayed bridges. Advances in Engineering Software 2009;40:830–5.
[31] Samui P. Application of statistical learning algorithms to ultimate bearing capacity of shallow foundation on cohesionless soil. Int

J Numer Anal Methods Geomech 2012;36:100–10.
[32] Rajasekaran S, Gayathri S, Lee T-L. Support vector regression methodology for storm surge predictions. Ocean Engineering 2008;35:1578–87.
[33] Gunn SR. Support vector machines for classification and regression. ISIS Technical Report 1998;14:5–16.
[34] Vapnik V, Golowich S, Smola A. Support vector method for function approximation, regression estimation and signal processing. Adv Neural Inf Process Syst 1996;9.
[35] Vapnik V. The nature of statistical learning theory. Springer science & business media; 1999.
[36] Al-Fugara A, Ahmadlou M, Al-Shabeeb AR, AlAyyash S, Al-Amoush H, Al-Adamat R. Spatial mapping of groundwater springs potentiality using grid search-based and genetic algorithm-based support vector regression. Geocarto Int 2020:1–20.
[37] Abualigah L, Diabat A, Mirjalili S, Abd Elaziz M, Gandomi AH. The Arithmetic Optimization Algorithm. Comput Methods Appl Mech Eng 2021;376:113609. doi:10.1016/j.cma.2020.113609.
[38] Mirjalili S. The ant lion optimizer. Advances in Engineering Software 2015;83:80–98.
[39] Saremi S, Mirjalili S, Lewis A. Grasshopper optimisation algorithm: theory and application. Advances in Engineering Software 2017;105:30–47.
[40] Golafshani EM, Pazouki G. Predicting the compressive strength of self-compacting concrete containing fly ash using a hybrid artificial intelligence method. Computers and Concrete, An International Journal 2018;22:419–37.
[41] B K A MAR, Ngamkhanong C, Wu Y, Kaewunruen S. Recycled Aggregates Concrete Compressive Strength Prediction Using Artificial Neural Networks (ANNs). Infrastructures (Basel) 2021;6:17. doi:10.3390/infrastructures6020017.